ELSEVIER

Journal of Structural Geology 26 (2004) 1749–1754

JOURNAL OF STRUCTURAL GEOLOGY

www.elsevier.com/locate/jsg

Can a Newtonian viscous-matrix model be applied to microboudinage of columnar grains in quartzose tectonites?

Toshiaki Masuda*, Nozomi Kimura

Institute of Geosciences, Shizuoka University, Shizuoka 422-8529, Japan

Received 25 August 2003; accepted 12 February 2004

Available online 17 July 2004

Abstract

A Newtonian viscous rheology was assumed for the matrix around the microboudins of columnar mineral grains in metamorphic tectonites, and a new expression was derived for predicting the proportion of boudinaged grains as a function of the aspect ratio of the columnar grains and the magnitude of far-field differential stress. The predicted proportion was compared with the measured proportions of tourmaline, piemontite and sodic amphibole in seven samples from various orogenic belts. The comparison revealed that the predictions were remarkably different from the measured values. This suggests that the viscous-matrix model cannot be applied to the stress state of the matrix during microboudinage.

Keywords: Elastic-matrix model; Microboudinage; Newtonian viscous-matrix model; Quartzose metamorphic tectonites; Stress analysis

1. Introduction

In studies on natural solid-state deformation from the microscopic to global scales, rocks and minerals are usually approximated as viscous materials. This is because it is easier to analyse viscous materials than solid-state materials theoretically and experimentally. For instance, Ramberg (1955) performed analogue-model experiments and viscous mechanical analyses to study boudinage of competent strata, MacKenzie (1979) simulated mantle convection by fluid dynamics, and Masuda and Ando (1988) analysed the deflection of viscous flow around a rigid spherical body. Experimental studies using a Newtonian viscous material also provide fruitful results (e.g. Weijermars, 1986; Passchier and Sokoutis, 1993; Arbaret et al., 2001; Mancktelow et al., 2002). The results of these studies are apparently all applicable to the interpretation of the strain patterns in natural deformation. However, solid-state deformation is significantly different from the Newtonian viscous state. Therefore, there is a need to evaluate if Newtonian viscous analysis is applicable to the solid-state deformation of rocks. In most cases we cannot reasonably accept or deny the applicability, because we have no suitable criteria by which to judge it. This paper analyses the stress state during the microboudinage of columnar mineral grains in metamorphic tectonites by which we can judge the applicability of the approach.

2. Stages in microboudinage

Consider microboudinage of competent columnar mineral grains in metamorphic tectonites (e.g. Misch, 1969; Masuda et al., 1989; Ji and Zhao, 1993). Fig. 1 shows typical examples of microboudins of tourmaline and sodic amphibole embedded within a quartzose matrix. The microboudinage of a competent grain into two separate segments (microboudins) can be well represented by the following three stages (Fig. 2): (1) before fracturing: the stress imposed on the rock matrix (far-field stress) is transferred to the competent grain to induce local stress; (2) fracturing: the competent grain fractures when the local stress generated in the grain exceeds the grain strength; and (3) separation: segments after fracturing are pulled apart within the matrix and the matrix material penetrates into the inter-boudin gaps. These three stages can repeat to form several microboudins from one single columnar grain when the applied stress continues to increase. If the stress decreases, the separation continues to form wider inter-boudin gaps but no new fracturing occurs. The microboudin

* Corresponding author. Tel.: +81-54-238-4794; fax: +81-54-238-0491.

0191-8141/$ - see front matter © 2004 Elsevier Ltd. All rights reserved.
doi:10.1016/j.jsg.2004.02.008

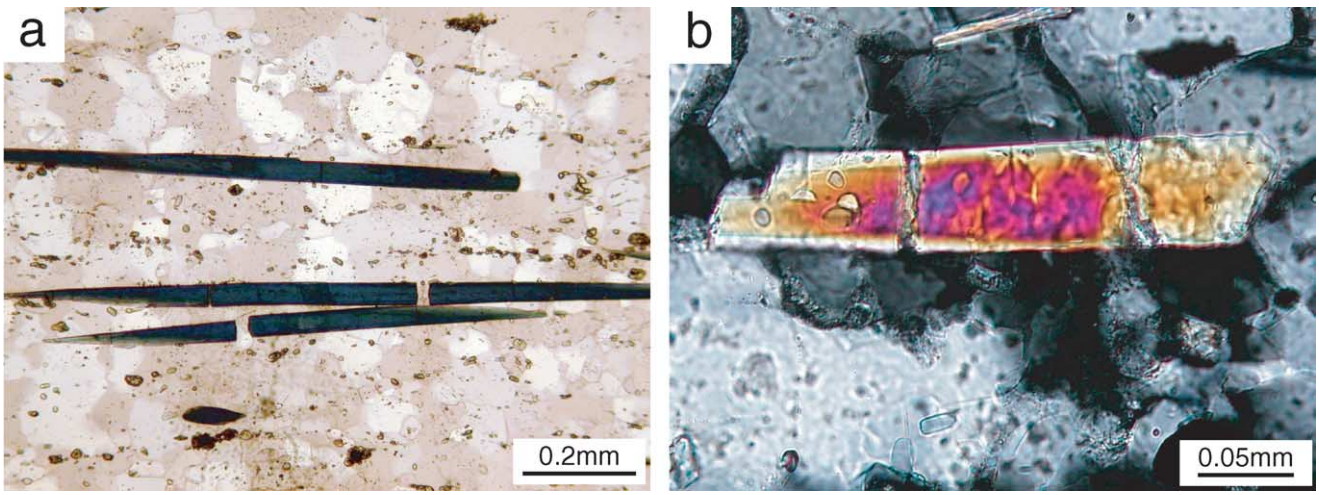

Fig. 1. Photomicrographs of the microboudinaged grains. (a) Sodic amphibole boudins from Aksu, China. (b) Tourmaline boudins from Wadi Tayin, Sultanate of Oman.

structures freeze when the matrix material ultimately ceases to flow due to the decrease in temperature (e.g. Masuda et al., 1990). As the matrix and the competent material are never molten during the three stages in the metamorphic processes, the microboudinage occurs purely in the solid-state. This paper is mainly concerned with the stages (1) and (2).

3. Basic data of microboudin structures for the stress analysis

Seven pre-analysed samples of metamorphic tectonites were re-used to test the applicability of the viscous matrix model. Masuda et al. (2003, 2004) presented tourmaline boudins from Greenbushes (latest Archaean, Western Australia) and Wadi Tayin (Cretaceous, Sultanate of Oman), piemontite boudins from four localities (Nuporomaporo, Yamagami, Asemi and Matsunosako) in Japan and sodic amphibole boudins from Aksu (late Proterozoic, NW China). The matrices of these seven samples are quartzose. The basic data for the applicability test consists of a proportion of boudinaged grains with respect to the aspect ratio of the columnar mineral grains. The frequency distributions of boudinaged and intact columnar grains are shown in Fig. 3, and the proportions of boudinaged grains

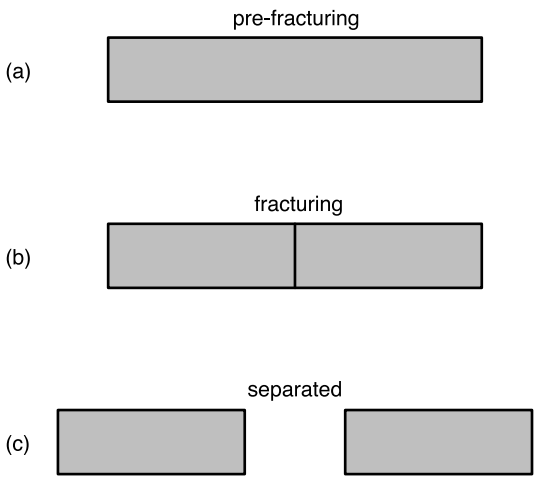

Fig. 2. Schematic drawing of microboudinage. (a) Pre-fracturing stage, (b) fracturing stage, (c) being-separated stage.

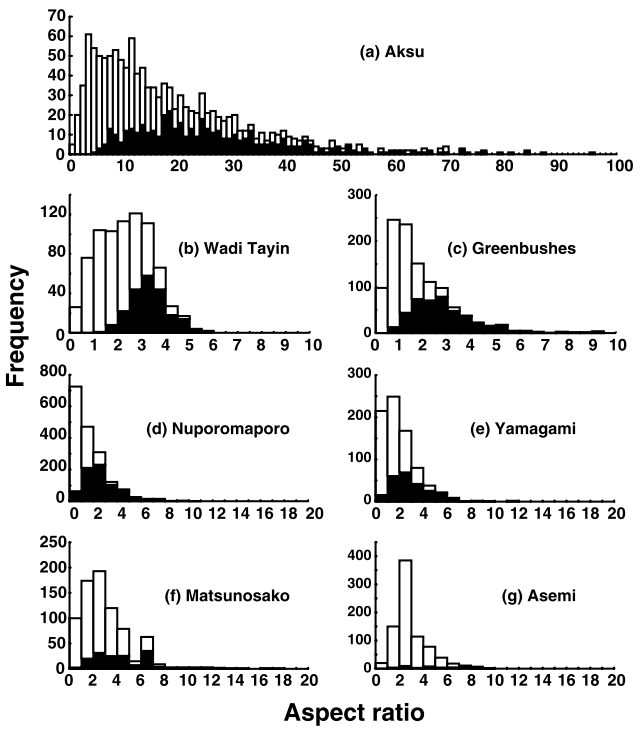

Fig. 3. Frequency distributions of boudinaged and intact columnar mineral grains. The data are reproduced from Masuda et al. (2003, 2004). (a) Sodic amphibole from Aksu, China, (b) tourmaline from Wadi Tayin, Sultanate of Oman, (c) tourmaline from Greenbushes, Australia, (d) piemontite from Nuporomaporo, Japan, (e) piemontite from Yamagami, Japan, (f) piemontite from Matsunosako, Japan, and (g) piemontite from Asemi, Japan.

are plotted in Fig. 4. The proportion is designated as $M(r)$ and used in later analysis.

4. Application of the viscous model to boudinage

Ramberg (1955) solved the stress-state in a competent layer subjected to one-dimensional elongation as a function of the strain rate of the surrounding Newtonian viscous matrix. The boudinage is caused by the drag force of the viscous matrix on the competent layer when the matrix flows along the layer (Fig. 5). The competent layer is assumed to be elastic before rupture. The relationship between the compressive strain rate of the matrix along the z-axis, $-\partial(z/z_i)/\partial t$, and the tensile stress within the competent layer, $\sigma(x)$ is expressed as:

$$\sigma(x) = \frac{6\mu}{z_c z_i^2}\left(-\frac{\partial z}{\partial t}\right)\left(l^2 - x^2\right) \tag{1}$$

where μ is viscosity of the matrix, and z_c and z_i are the thickness of competent layer and matrix, respectively, l is the half-length of the layer, and x is the distance from the centre of the layer perpendicular to the expected fracture plane (Ramberg, 1955, p. 524). The width of the layer (y)

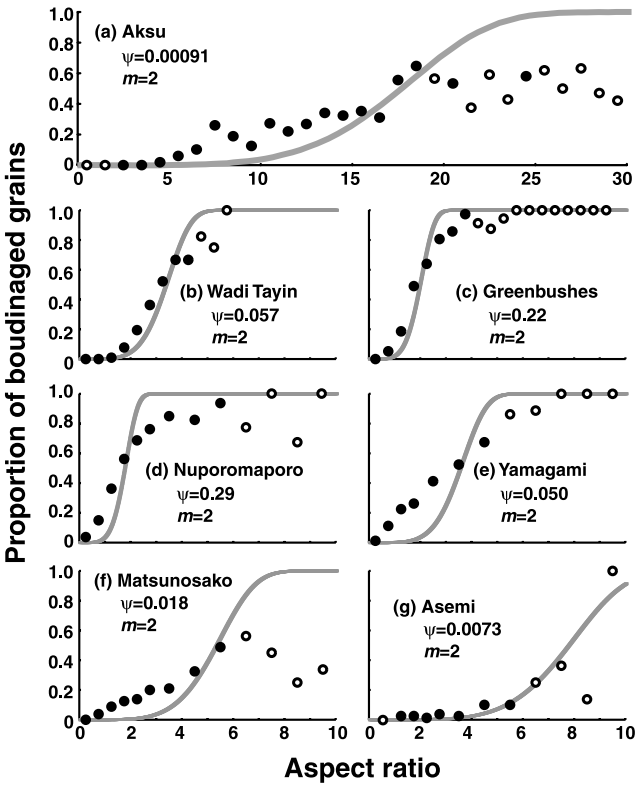

Fig. 4. Proportion of boudinaged grains with respect to aspect ratio. The plotted data are reproduced from Masuda et al. (2003, 2004). For the data from (a)–(g), see Fig. 3. Solid and open circles indicate reliable and unreliable data (>25 measured grains are regarded as reliable). The curve represents the best-fit $G_v(r, \psi)$ using reliable data. Each λ-value is indicated.

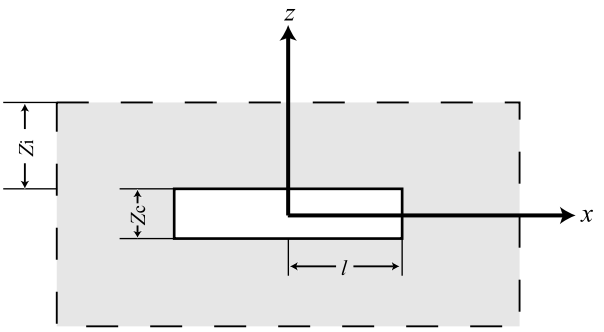

Fig. 5. Setting of the Newtonian viscous model simplified after Ramberg (1955). The simplification is guaranteed by the fact that the width of the boudinaged layer does not affect the magnitude of stress in the layer (Ramberg, 1955). For parameters see Appendix A.

does not affect the magnitude of the stress. The strain rate is related to the far-field differential stress (σ_0) as:

$$\sigma_0 = \frac{\mu}{z_i}\left(-\frac{\partial z}{\partial t}\right) \tag{2}$$

Thus, substituting Eq. (2) into Eq. (1), a simple equation that encompasses the local stress in the competent layer and far-field stress is derived as:

$$\sigma(x) = \frac{6\sigma_0}{z_c z_i}\left(l^2 - x^2\right) \tag{3}$$

5. Derivation of a new probability distribution function of fracturing

Eq. (3) can be modified to predict the proportion of boudinaged grains with respect to the aspect ratio of columnar mineral grains in a manner that is similar to that presented by Masuda et al. (2003) as follows. The maximum tensile stress occurs at the centre of the layer ($x = 0$), and the value (σ) is given by

$$\sigma = \frac{6\sigma_0 l^2}{z_c z_i} \tag{4}$$

As fracturing usually occurs in the central part of the grain (see Masuda and Kuriyama, 1988), this value of stress is regarded as being representative for subsequent analysis.

The aspect ratio (r) of the competent layer is given by:

$$r = \frac{2l}{z_c} \tag{5}$$

By using Eqs. (4) and (5), the relationship between the stress and the aspect ratio is simply written as:

$$\sigma = Kr^2 \tag{6}$$

where

$$K = \frac{3\sigma_0 z_c}{2z_i} \tag{7}$$

K is regarded as a parameter proportional to the far-field stress, σ_0.

The fracturing of competent grains is described statistically. The weakest-link theory (e.g. Weibull, 1939; Epstein, 1948; Masuda et al., 2003, 2004) shows that the probability distribution function of fracture strength, $G_v(r,\ \sigma)$, is given as a function of r and σ:

$$G_v(r,\ \sigma) = 1 - \exp\left[-\frac{m-1}{m} r \left(\frac{\sigma}{S^*} \right)^m \right] \tag{8}$$

where m is the Weibull modulus and S^* is the modal fracture strength of the competent material at $r = 1$: m and S^* are regarded as constants depending on materials. By substituting Eq. (6) into Eq. (8), we obtain:

$$\begin{aligned} G_v(r,\ \sigma) &= 1 - \exp\left[-\frac{m-1}{m} r \left(\frac{Kr^2}{S^*} \right)^m \right] \\ &= 1 - \exp\left[-\frac{m-1}{m} r^{2m+1} \left(\frac{K}{S^*} \right)^m \right] \end{aligned} \tag{9}$$

A new dimensionless stress parameter ψ is introduced as:

$$\psi = \frac{K}{S^*} = \frac{3}{2} \frac{z_c}{z_i} \frac{\sigma_0}{S^*} \tag{10}$$

By using ψ, the probability distribution function finally becomes:

$$G_v(r,\ \sigma) = 1 - \exp\left[-\frac{m-1}{m} r^{2m+1} \psi^m \right] \tag{11}$$

6. Determination of the stress parameter ψ

The proportion of boudinaged grains was measured independently with respect to the aspect ratio of the boudin materials, $M(r)$. $M(r)$ is a natural data set compared with $G_v(r,\ \sigma)$. The value of ψ can be determined by the method of least-squares. $T(\psi)$ is defined as:

$$T(\psi) = \sum_r \left[G_v(r,\ \psi) - M(r) \right]^2 \tag{12}$$

and ψ is obtained so as to minimize $T(\psi)$. However, m in Eq. (11) is also unknown and is regarded as a parameter to be obtained. The value of m and ψ are determined so as to minimize $T(m,\ \psi)$:

$$T(m,\ \psi) = \sum \left[G_v(r,\ m,\ \psi) - M(r) \right]^2 \tag{13}$$

The obtained values of m and ψ and the best-fit $G_v(r,\ m,\ \psi)$ for each sample are shown in Fig. 4.

7. Evaluation of fitting: is the viscous-matrix model applicable?

The fit of $G_v(r,\ m,\ \psi)$ to $M(r)$ appears inappropriate, as shown in Fig. 4. The fit was evaluated using the χ^2-test (Cheeney, 1983) and the results showed that the fitting is not appropriate statistically. Thus, it is obvious that the Newtonian viscous-matrix model cannot well express the stress state in columnar mineral grains embedded within the solid-state matrix.

8. Applicability of the elastic-matrix model

In contrast, the elastic-matrix model (shear-lag model of e.g. Zhao and Ji, 1997) was successfully applied to the microboudinage structures of the seven samples as shown in Masuda et al. (2003, 2004). The principal of the method is that the solid matrix elastically transmits the far-field stress to the fibre minerals (e.g. Lloyd et al., 1982; Zhao and Ji, 1997; Masuda et al., 2003, 2004), and that the theoretically derived probability distribution of the fracturing of fibre-grains is described by $G(r,\ \lambda)$ as a function of the aspect ratio (r) and the far-field differential stress (σ_0) as:

$$G(r,\ \lambda) = 1 - \exp\left[-\frac{m-1}{m} r \lambda^m \left(\frac{E_f}{E_q} \right)^m \left\{ 1 - \left(1 - \frac{E_q}{E_f} \right) \frac{1}{\cosh(Ar)} \right\}^m \right] \tag{14}$$

where E_q and E_f are the elastic constants of the matrix and fibre, respectively, and A is a constant. λ is defined as:

$$\lambda = \frac{\sigma_0}{S^*} \tag{15}$$

As in the viscous-matrix model, the theoretical and measured values were compared. The best-fit results in Fig. 6 are reproduced from Masuda et al. (2003, 2004). The validity of the fitting was proved statistically in Masuda et al. (2003, 2004). This figure shows that the elastic-matrix model can be successfully applied to the microboudinage.

9. Discussion and implications

The Newtonian viscous-matrix model cannot simulate the stress-state during microboudinage, whereas the elastic-matrix model was successfully applied to the microboudinage structures. As the microboudinage took place in the solid-state during metamorphism, this result is understandable and acceptable.

There may be many other cases in which viscous theory appears to be successfully applied and thereby promotes misunderstanding. In order to prevent this from occurring, we must understand the limits of the applicability of the

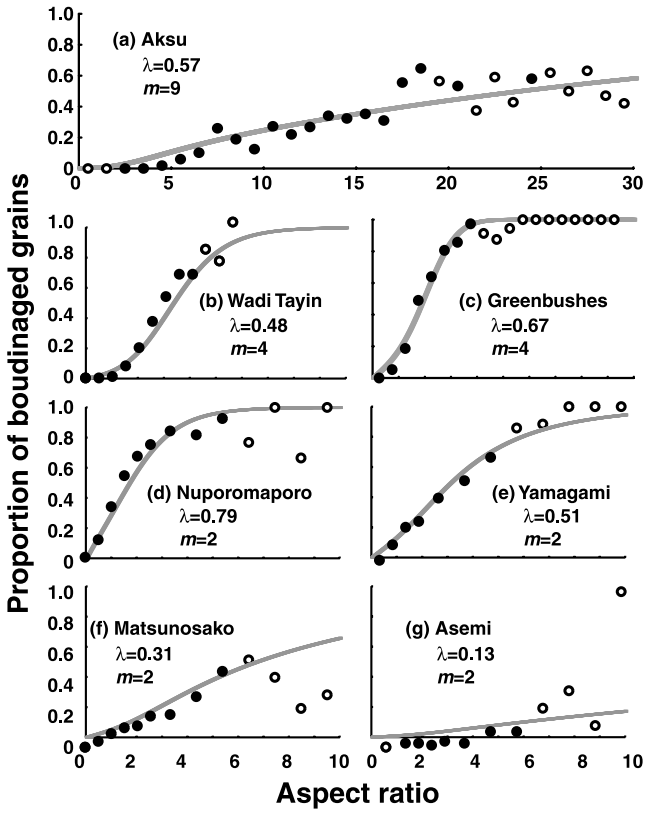

Fig. 6. Fitting the microboudin data of Fig. 4 using the elastic-matrix model. The plotted data are the same as Fig. 4. The solid curves represent the best-fit $G(r, \lambda)$.

viscous model to solid-state deformation. Our knowledge of the difference between 'viscous' and 'solid-state' remains incomplete.

Acknowledgements

The authors thank Shohei Banno and Mitsuhiro Toriumi, Shaocheng, Ji and an anonymous reviewer for their encouragement on our study. The authors also thank Hideki Mori for preparing thin sections. This study was financially supported by the Japan Society for the Promotion of Science.

Appendix A. Notations

x, y and z: Cartesian coordinates
μ: Newtonian viscosity
z_c: thickness of competent layer
z_i: thickness of matrix
l: half length of competent layer
σ: differential stress within competent layer
σ_0: far-field differential stress
$-\partial(z/z_i)/\partial t$: compressional strain rate along the z axis
r: aspect ratio of columnar mineral grain
K: a parameter proportional to σ_0
G_v: probability distribution function of fracturing based on the viscous-matrix model
S^*: fracture strength of boudin material
m: Weibull modulus
M: measured proportion of boudinaged grains
T: square difference between G_v and M
ψ: stress parameter based on viscous-matrix model
G: probability distribution function of fracturing based on the elastic-matrix model
λ: stress parameter for elastic-matrix model
E_q: Young's modulus of matrix
E_f: Young's modulus of columnar mineral
A: a constant

References

Arbaret, L., Mancktelow, N., Burg, J.-P., 2001. Effect of shape and orientation on rigid particle orientation and matrix deformation in simple shear flow. Journal of Structural Geology 23, 113–125.
Cheeney, R.F., 1983. Statistical Methods in Geology, George Allen & Unwin, London.
Epstein, B., 1948. Statistical aspects of fracture problems. Journal of Applied Physics 19, 140–147.
Ji, S., Zhao, P., 1993. Location of tensile fracture within rigid-brittle inclusions in ductile flowing matrix. Tectonophysics 220, 23–31.
Lloyd, G.E., Ferguson, C.C., Reading, K., 1982. A stress-transfer model for development of extension fracture boudinage. Journal of Structural Geology 4, 355–372.
MacKenzie, D., 1979. Finite deformation during fluid flow. Geophysical Journal of Royal Astronomical Society 58, 687–715.
Mancktelow, N., Arbaret, L., Pennacchioni, G., 2002. Experimental observations on the effect of interface slip on rotation and stabilisation of rigid particles in simple shear and a comparison with natural mylonites. Journal of Structural Geology 24, 567–585.
Masuda, T., Ando, S., 1988. Viscous flow around a rigid spherical body: a hydrodynamical approach. Tectonophysics 148, 337–346.
Masuda, T., Kuriyama, M., 1988. Successive "mid-point" fracturing during microboudinage: an estimate of the stress-strain relation during a natural deformation. Tectonophysics 147, 171–177.
Masuda, T., Shibutani, T., Igarashi, T., Kuriyama, M., 1989. Microboudin structure of piedmontite in quartz schists: a proposal for a new indicator of relative palaeodifferential stress. Tectonophysics 163, 169–180.
Masuda, T., Shibutani, T., Kuriyama, M., Igarashi, T., 1990. Development of microboudinage: an estimate of changing differential stress with increasing strain. Tectonophysics 178, 379–387.
Masuda, T., Kimura, N., Hara, Y., 2003. Progress in microboudin method for palaeo-stress analysis of metamorphic tectonites: application of mathematically refined expression. Tectonophysics 464, 1–8.
Masuda, T., Kimura, N., Fu, B., Li, X., 2004. Validity of the microboudin method for palaeo-stress analysis: application to extraordinarily long sodic amphibole grains in a metachert from Aksu, China. Journal of Structural Geology, 26, 203–206.
Misch, P., 1969. Paracrystalline microboudinage of zoned grains and other criteria for synkinematic growth of metamorphic minerals. American Journal of Science 267, 43–63.
Passchier, C.W., Sokoutis, D., 1993. Experimental modelling of mantled porphyroclasts. Journal of Structural Geology 15, 895–909.
Ramberg, H., 1955. Natural and experimental boudinage and pinch-and-swell structures. Journal of Geology 63, 512–526.

Weibull, W., 1939. Statistical theory of the strength of materials. Ingeniors Vetenskaps Akademiens Handlingar 151 (cited in Epstein, 1948).
Weijermars, R., 1986. Flow behaviour and physical chemistry of bouncing putties and related polymers in view of tectonic laboratory applications. Tectonophysics 124, 325–358.
Zhao, P., Ji, S., 1997. Refinements of shear-lag model and its applications. Tectonophysics 279, 37–53.